



Published in final edited form as:

*J Control Release*. 2021 May 10; 333: 176–187. doi:10.1016/j.jconrel.2021.03.032.

## Self-assembled elastin-like polypeptide fusion protein coacervates as competitive inhibitors of advanced glycation end-products enhance diabetic wound healing

Hwan June Kang<sup>a</sup>, Suneel Kumar<sup>a</sup>, Arielle D'Elia<sup>a</sup>, Biraja Dash<sup>b</sup>, Vikas Nanda<sup>c</sup>, Henry C. Hsia<sup>b</sup>, Martin L. Yarmush<sup>a</sup>, François Berthiaume<sup>a,\*</sup>

<sup>a</sup>Department of Biomedical Engineering, Rutgers University, Piscataway, NJ 08854, USA

<sup>b</sup>Department of Surgery (Plastic), Yale School of Medicine, New Haven, CT 06510, USA

<sup>c</sup>Department of Biochemistry and Molecular Biology, Robert Wood Johnson Medical School, Center for Advanced Biotechnology and Medicine, Rutgers University, Piscataway, NJ 08854, USA

### Abstract

Chronic and non-healing skin wounds are some of the most significant complications in patients with advanced diabetes. A contributing mechanism to this pathology is the non-enzymatic glycation of proteins due to hyperglycemia, leading to the formation of advanced glycation end products (AGEs). AGEs bind to the receptor for AGEs (RAGE), which triggers pro-inflammatory signals that may inhibit the proliferative phase of wound healing. Soluble forms of RAGE (sRAGE) may be used as a competitive inhibitor of AGE-mediated signaling; however, sRAGE is short-lived in the highly proteolytic wound environment. We developed a recombinant fusion protein containing the binding domain of RAGE (vRAGE) linked to elastin-like polypeptides (ELPs) that self-assembles into coacervates at around 30–31 °C. The coacervate size was concentration and temperature-dependent, ranging between 500 and 1600 nm. vRAGE-ELP reversed several AGE-mediated changes in cultured human umbilical vein endothelial cells, including a decrease in viable cell number, an increase in levels of reactive oxygen species (ROS), and an increased expression of the pro-inflammatory marker, intercellular adhesion molecule-1 (ICAM-1). vRAGE-ELP was stable in elastase *in vitro* for 7 days. When used in a single topical application on full-thickness excisional skin wounds in diabetic mice, wound closure was accelerated, with 90% and 100% wound closure on post-wounding days 28 and 35, respectively, compared to 62% and 85% on the same days in animals treated with vehicle control, consisting of ELP alone. This coacervate system topically delivering a competitive inhibitor of AGEs has potential for the treatment of diabetic wounds.

\*Corresponding author at: Biomedical Engineering, 599 Taylor Road, Piscataway, NJ 08854, USA. fberthia@soe.rutgers.edu (F. Berthiaume).

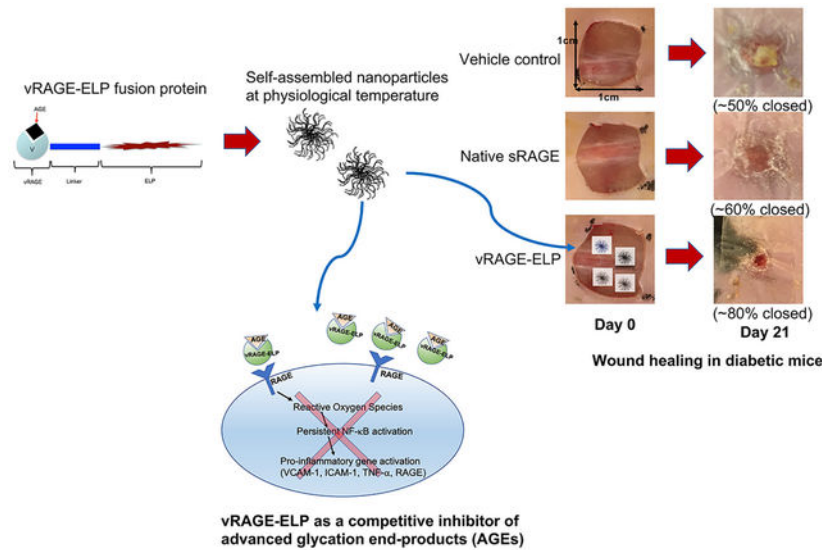
#### Declaration of Competing Interest

The authors declare that they have no known competing financial interests or personal relationships that could have appeared to influence the work reported in this paper.

#### Appendix A. Supplementary data

Supplementary data to this article can be found online at <https://doi.org/10.1016/j.jconrel.2021.03.032>.

## Graphical Abstract



## Keywords

Diabetic foot ulcer; Self-assembled coacervates; Elastin-like polypeptide; Advanced glycation end-product; Chronic skin wounds

## 1. Introduction

Four to ten percent of diabetic patients develop a diabetic foot ulcer (DFU) each year [1] and total Medicare spending estimates for DFUs range between \$6.2 and \$18.7 billion yearly in the U.S. [2]. DFUs are chronic wounds in which the normal wound healing process is impaired due to diabetes-related mechanisms [3]. Protein glycation due to the diabetic hyperglycemic environment is potentially a major factor underlying the pathology of slow healing of diabetic wounds [3]. Protein glycation occurs when free amino groups of proteins react with carbonyl groups on reactive sugars leading to the formation of advanced glycation end-products (AGEs), which triggers pro-inflammatory signals that may inhibit the proliferative phase of wound healing [4,5].

AGEs bind their cognate receptors (RAGEs) found on endothelial cells, macrophages, as well as mesangial cells [6]. AGE-RAGE binding induces intracellular generation of reactive oxygen species (ROS), which in turn results in the activation of the nuclear transcription factor, NF- $\kappa$ B, an inducer of pro-inflammatory gene expression [7,8]. Among those are vascular cell adhesion molecule 1 (VCAM-1), intercellular adhesion molecule 1 (ICAM-1), tumor necrosis factor alpha (TNF- $\alpha$ ) and metalloproteinases (MMPs) [9–11]. Furthermore, AGE-RAGE binding upregulates the expression of RAGE itself which then contributes to prolonged inflammation [4].

Soluble RAGEs (sRAGE) lacking the transmembrane and cytoplasmic domains of RAGEs could act as a competitive inhibitor of AGEs. In prior studies, application of sRAGE reduced

pro-inflammatory gene expression, enhanced wound healing in diabetic animal models, and recovered the bioactivity of stromal cell derived factor 1 (SDF-1), which supports re-epithelialization during wound healing, in *in vitro* diabetic environments [11–13]. Among the five domains of RAGEs (V, C1, C2, transmembrane and cytoplasmic domains), the extracellular V domain is the one that binds AGEs [14,15]. Several studies have found that an application of recombinant V domain of RAGE (vRAGE) blocked AGE-RAGE binding *in vitro* [10,16]. While sRAGE and vRAGE could be used as potential therapeutic peptides, they are subject to degradation in the presence of proteases. In fact, higher levels of MMPs have been reported in chronic wounds compared to acute wounds, and specifically in diabetic wounds, high levels of MMP-2 and MMP-9 have been found [17]. Topical application of growth factors is under consideration to compensate for decreased activities of growth factors in chronic wounds [18]. However, exogenous growth factors have not been very successful as therapeutic agents, presumably due to their rapid degradation in the highly proteolytic chronic wound environment, which similarly affect other bioactive peptides [18].

Elastin-like polypeptides (ELPs) that can be expressed as a fusion protein with various bioactive peptides to create coacervates have been shown to serve as “shields” from exposure to the highly proteolytic environment [19–23]. ELPs are derivatives of tropoelastin consisting of pentapeptide repeats of Valine-Proline-Glycine-Xaa-Glycine, where Xaa can be any amino acids except Proline [24,25]. ELPs are thermally responsive and reversibly self-assemble into coacervates above a transition temperature [26]. In the present study, we have developed a self-assembled coacervate system containing a fusion of vRAGE and ELPs (vRAGE-ELP) that effectively blocks AGE-RAGE-mediated signaling, thus improving diabetic wound healing.

## 2. Materials and methods

### 2.1. Design and cloning of a vRAGE-ELP expression vector

DNA encoding the V domain (residues 23–123) [15] of RAGE that contains *XbaI* and *NdeI* restriction enzyme sites and a short linker sequence of three repeats of four glycines and one serine was synthesized and ordered from GenScript Biotech (Piscataway, NJ, USA). Previously, a pET25B+ plasmid encoding 50 pentapeptide repeats of ELP and a 6-histidine tag was used to develop a fusion protein containing SDF1 and ELP [23,27]. The same pET25B+ plasmid with ELP repeats was used to subclone the V domain genes into the ELP expression vector using the two restriction enzyme sites, *XbaI* and *NdeI*. The subcloning of vRAGE-ELP expression vector and sequencing of the ligation areas were performed by GenScript to ensure a successful cloning of the vRAGE-ELP expression vector.

### 2.2. Expression of vRAGE-ELP fusion protein and empty ELP protein

*E. coli* (One Shot™ BL21 Star™ (DE3) Chemically Competent, Invitrogen™) was purchased from Thermo Fisher Scientific (USA). The bacterial cells were transformed with the vRAGE-ELP expression vector by following the manufacturer's instructions. The transformation reaction was plated onto LB agar plate containing 100 µg/mL of carbenicillin and incubated overnight at 37 °C. Next day, a single, isolated colony was picked. The colony

was then inoculated in 25 mL of LB medium containing 100 µg/mL of carbenicillin by shaking overnight at 220 rpm at 37 °C. The 25 mL overnight culture was then transferred to 1 L of TB medium containing 100 µg/mL of carbenicillin, and the culture was grown by shaking at 220 rpm at 37 °C until the optical density (OD) reached 0.6–0.8. When the OD reached 0.6–0.8, 1 mM of isopropyl β-d-1-thiogalactopyranoside (IPTG, Gold Biotechnology, USA) was added to induce protein expression and the culture was left overnight at 37 °C by shaking at 220 rpm. Next day, the overnight culture was collected in four 250 mL bottles and centrifuged at 3000 *g* for 20 min at 4 °C. The supernatant was discarded, and the bacterial pellets were stored at –80 °C until ready for purification. Similarly, empty ELP proteins without the vRAGE insert were expressed to be used as a vehicle control.

### 2.3. Purification of vRAGE-ELP fusion protein and empty ELP protein

The thermally responsive property of ELP was used to purify the proteins as previously described [22,23,25]. Briefly, the bacterial pellets from the 1 L culture were resuspended in a total of 28 mL of cold phosphate buffered saline (PBS) and sonicated on ice for 3 min (5 s ON, 25 s OFF cycle) twice. Poly(ethyleneimine) (PEI) solution (MilliporeSigma, USA) at a final concentration of 0.5% *w/v* was added to the cell lysate to remove negatively charged residual DNA. The cell lysate was then centrifuged at 18,000 *g* for 15 min at 4 °C and the supernatant containing the fusion proteins was collected in a new 50 mL conical tube. 0.3 M of sodium citrate (MilliporeSigma, USA) was added to the protein solution to induce coacervate formation followed by incubating in a 35 °C water bath for 10 min. The protein sample was centrifuged at 16,000 *g* for 10 min at 35 °C (1st “hot spin”). 20 µL of supernatant containing soluble contaminants were collected for SDS-PAGE analysis, and the protein pellet containing the vRAGE-ELP fusion protein was resuspended in ~5 mL of icy cold PBS to resolubilize the fusion protein. The tube was placed on ice and occasionally vortexed until the pellet was completely dissolved. The tube was then centrifuged at 16,000 *g* for 10 min at 4 °C (1st “cold spin”). 20 µL of the supernatant containing soluble vRAGE-ELP fusion proteins were saved for SDS-PAGE analysis and a pellet containing insoluble contaminants was discarded. The procedures of “hot spin” and “cold spin” were repeated three times to obtain pure vRAGE-ELP fusion proteins at the end of process. Empty ELP proteins were purified using similar methods.

### 2.4. Physical characterization

**2.4.1. SDS-PAGE and Western blot**—The samples collected after each hot and cold spin during the purification process were run on SDS-PAGE using 4–20% precast gel and Tris/Glycine/SDS buffer (Bio-Rad Laboratories, USA) to separate proteins by size. The gel was stained with SimplyBlue™ SafeStain solution (Thermo Fisher Scientific) for 1 h to visualize protein bands followed by washing in distilled water for 1 h. In a separate experiment, an SDS-PAGE gel was transferred onto a nitrocellulose membrane (0.2 µm pore size, Bio-Rad Laboratories) for Western blotting. The membrane was then blocked with 1× TBS 1× casein blocker (Bio-Rad Laboratories) for one hour. After the blocking step, the membrane was incubated with anti-RAGE antibody (ab37647, Abcam, USA) overnight at 4 °C. Next day, the membrane was washed three times with PBS containing 0.05% Tween 20 (PBST) for 5 min each. The membrane was then incubated with HRP conjugated secondary

antibody (Goat Anti-Rabbit IgG, (H + L), HRP conjugated, Thermo Fisher Scientific) for 1 h at room temperature. The membrane was washed with PBST three times and exposed to TMB substrate solution (1-Step™ Ultra TMB-Blotting Solution, Thermo Fisher Scientific).

**2.4.2. Quantification of bacterial endotoxin level**—To quantify bacterial endotoxin levels in the purified fusion protein, a chromogenic limulus amoebocyte lysate (LAL) assay (ToxinSensor™ Chromogenic LAL Endotoxin Assay Kit, GenScript) was used according to the manufacturer's protocol.

**2.4.3. Measurement of solution turbidity**—25 μM of purified vRAGE-ELP fusion proteins in PBS (100 μL total volume) were prepared in a 96-well plate. The plate was placed in a plate reader to measure the turbidity of the protein solution as the temperature of the instrument was increased from an initial temperature of 22 °C to a final temperature of 40 °C in 1 °C increments. Solution turbidity, which indicates the formation of coacervates above the transition temperature, was determined by measuring the absorbance of the samples at 350 nm.

**2.4.4. Size of coacervates**—Three different concentrations of vRAGE-ELP fusion proteins (5 μM, 10 μM and 25 μM) in 25 μL of PBS were prepared to measure the sizes of coacervates. The size was measured at 4 °C, 30 °C, and 37 °C by dynamic light scattering using a Zetasizer Nano S (Malvern Panalytical, USA). The size of coacervates over time was also monitored by incubating vRAGE-ELP at 5 μM at 37 °C and collecting samples at days 0, 1, 3, 5 and 7. The size of each sample was measured by dynamic light scattering.

**2.4.5. Binding activity of vRAGE-ELP to AGE**—A commercially available AGE-RAGE *in vitro* binding assay kit (CircuLex AGE-RAGE *in vitro* Binding Assay Kit, MBL International Corporation, USA) was used to investigate the binding ability of vRAGE-ELP to AGE according to the manufacturer's protocol with a slight modification. Briefly, vRAGE-ELP fusion proteins, recombinant sRAGE, and empty ELP, all of which contain a 6-histidine tag, were prepared in reaction buffer at various concentrations. vRAGE-ELP, sRAGE or ELP was then added to an AGE (glycated BSA)-coated well in a 96-well plate or a BSA-coated well in a 96-well plate as a control. The plates were incubated for 60 min at room temperature after which the wells were washed with wash buffer four times. After washing, HRP conjugated anti-His-tag antibody was added and the plates were incubated for 60 min. The plates were then washed four times with wash buffer. Substrate reagent was then added to each well and the plates were incubated for 10 min after which stop solution was added. The absorbance was measured at 450 nm.

**2.4.6. vRAGE-ELP monomer release from coacervates**—25 μM of vRAGE-ELP fusion protein (500 μL total volume) were prepared in each of six centrifugal tubes with 10 nm pore membranes (Nanosep® with Omega™ 100 K, Pall Corporation, USA). The tubes were equilibrated at 37 °C for 10 min to initiate coacervate formation. Subsequently, tubes were retrieved from incubation after 0, 1, 2, 4, 6 and 24 h of further incubation and immediately centrifuged at 5000 *g* for 5 min at 37 °C to separate protein monomers in filtrate from coacervates remaining on the membrane. The filtrate was collected in a new

tube and the proteins in filtrate was quantified using a bicinchoninic acid (BCA) assay (Thermo Fisher Scientific).

## 2.5. In vitro bioactivity

**2.5.1. Cell culture**—Primary human umbilical vein endothelial cells (HUVECs) were purchased from Thermo Fisher Scientific. Cells were maintained in M200 media supplemented with low serum growth supplement (LSGS) kit (Thermo Fisher Scientific).

**2.5.2. HUVEC viable number assay**—HUVECs were plated in a 96-well plate at a density of 2000 cells/well. Cells were grown in M200 media supplemented with LSGS kit overnight to allow for cell attachment. Next day, one group of cells was exposed to 100 µg/mL of bovine serum albumin (BSA, MilliporeSigma) as a control. Another group was stimulated with 100 µg/mL of commercially available AGEs consisting of glycated BSA (Advanced Glycation End Product-BSA, MilliporeSigma) to mimic a diabetic condition [9]. As previously done in the literature [10,28], for the treatment groups, 100 µg/mL of AGEs were pre-incubated with various concentrations of vRAGE-ELPs (300 µg/mL, 500 µg/mL or 1 mg/mL) or empty ELPs (300 µg/mL, 500 µg/mL or 1 mg/mL) for at least 30 min at 37 °C to allow enough time for the vRAGE-ELP coacervates to react with AGEs. Each mixture of AGEs and vRAGE-ELP coacervates was then added to cells in growth media. In the other group, cells were stimulated with AGEs and co-treated with 30 mM of *N*-acetylcysteine (NAC) as a treatment control. All groups were incubated for 24 h at 37 °C. Viable cell number per well was measured using a 3-(4,5-dimethylthiazol-2-yl)-2,5-diphenyl-2H-tetrazolium bromide (MTT) assay (Vybrant MTT cell proliferation assay kit, Thermo Fisher Scientific).

**2.5.3. ROS measurements**—HUVECs were plated in a 96-well plate at a density of 5000 cells/well in M200 media supplemented with LSGS kit and grown at 37 °C for 24 h. Cells were then treated with BSA (100 µg/mL), AGE (100 µg/mL) only, AGE (100 µg/mL) + vRAGE-ELP (1 mg/mL) (pre-incubated for 30 min), AGE (100 µg/mL) + ELP (1 mg/mL) (pre-incubated for 30 min), or AGE (100 µg/mL) + NAC (30 mM) and incubated at 37 °C for 24 h. To visualize the generation of intracellular ROS, CellRox<sup>®</sup> Green Reagent (Thermo Fisher Scientific) was used. Briefly, after 24 h of treatment, cells were washed with growth media twice to remove vRAGE-ELP coacervates from the well. CellRox<sup>®</sup> Green Reagent was then added to the cells in growth media at a final concentration of 5 µM and incubated at 37 °C. After 30 min, cells were washed three times with PBS. The intracellular ROS was visualized under the fluorescent microscope (Olympus IX81) and the images were captured.

## 2.5.4. Measurements of ICAM-1 expression

**2.5.4.1. Immunocytochemistry:** 8 mm cover glasses (Electron Microscopy Sciences, USA) were placed in a 48-well plate and coated with 0.1% gelatin in deionized water (MilliporeSigma) for 10 min at room temperature. The gelatin solution was removed, and the cover glasses were air-dried for 15 min before use. HUVECs were seeded onto cover glasses at a density of 5000 cells/well and grown in growth media. When cells became confluent, cells were treated with BSA (100 µg/mL), AGE (100 µg/mL) only, AGE (100 µg/mL) + vRAGE-ELP (1 mg/mL) (pre-incubated for 30 min), AGE (100 µg/mL) +

ELP (1 mg/mL) (pre-incubated for 30 min), or AGE (100 µg/mL) + NAC (30 mM) and incubated at 37 °C for 6 h. Cells were then washed with fresh media twice and fixed in 2% paraformaldehyde in PBS for 20 min at room temperature. Fixed cells were washed twice in wash buffer (0.1% BSA in PBS). Cells were then blocked with blocking buffer (10% normal donkey serum, 0.3% Triton X-100, MilliporeSigma) for 45 min at room temperature. After blocking, cells were incubated with human ICAM-1/CD54 antibody (R&D Systems, Catalog #BBA3) at a final concentration of 25 µg/mL for 1 h at room temperature. Cells were washed twice with wash buffer and incubated again with secondary antibody (Alexa Flour 647 donkey anti-mouse secondary antibody, Invitrogen # A-31571) for 1 h at room temperature. Cells were washed twice with wash buffer and a drop of antifade mounting medium containing DAPI (ProLong Diamond Antifade Mountant with DAPI, Invitrogen™) was added to each cover glass. Cover glasses were taken out of the well plate carefully using a tweezer and placed on glass slides. The expression of ICAM-1 was visualized by fluorescence microscopy (Olympus IX81) and the images were captured.

**2.5.4.2. Cell-based ELISA.:** HUVECs were plated in a 96-well plate at a density of 5000 cells/well and grown in growth media for 48 h or until confluence. When cells became confluent, cells were treated with BSA (100 µg/mL), AGE (100 µg/mL) only, AGE (100 µg/mL) + vRAGE-ELP (1 mg/mL) (pre-incubated for 30 min), AGE (100 µg/mL) + ELP (1 mg/mL) (pre-incubated for 30 min), AGE (100 µg/mL) + NAC (30 mM) or AGE (100 µg/mL) + Human RAGE antibody (10 µg/mL, R&D Systems, MAB11451) and incubated at 37 °C for 6 h. Cells were then washed with fresh media twice and fixed in 2% paraformaldehyde in PBS for 20 min at room temperature. Fixed cells were washed twice with PBS. Unspecific binding sites were blocked by incubating cells with blocking buffer containing 2% BSA and 4% non-fat dry milk for 30 min at room temperature. Cells were then incubated with anti-ICAM1 monoclonal antibody (Thermo Fisher Scientific, #MEM-111) diluted in blocking buffer for 2 h at 37 °C and washed four times with PBS. Cells were incubated with rabbit anti-mouse IgG HRP (Abcam, #ab6728) for 1 h at 37 °C and washed 5 times with PBS. After washing, TMB substrate (1-Step™ Ultra TMB-ELISA Substrate Solution, Thermo Fisher Scientific) was added to each well and colors were developed for 10 min at room temperature after which stop solution (Thermo Fisher Scientific, #N600) was added. Absorbance at 450 nm was measured to quantify the expression of ICAM-1.

**2.5.5. Stability test in the presence of elastase in vitro—**To investigate whether vRAGE-ELP remains stable in the presence of elastase (MilliporeSigma), we incubated 5 µM of vRAGE-ELP or free sRAGE in 1 µM of elastase or in PBS without elastase as a control at 37 °C for 1, 3, 5, and 7 days. Samples collected at each time point were stored in –80 °C until running on Western blot using the same method described above.

## 2.6. In vivo bioactivity: effects on wound healing in diabetic mice

**2.6.1. Wound closure study—**Animal studies were conducted in accordance with a protocol approved by the Institutional Animal Care and Use Committee (IACUC) at Rutgers University. Genetically modified diabetic mice (BKS. Cg-Dock7<sup>m+/+</sup> Lepr<sup>db/J</sup>, 3 females, 5 males) were purchased from the Jackson Laboratory (Bar Harbor, ME, USA) and used at the

age of 10 weeks. A day before surgery, mice were anesthetized by isoflurane (Henry Schein, USA) inhalation. The dorsum was shaved using a clipper, and Nair™ cream was applied to remove residual hair. On the day of surgery, a 1 cm by 1 cm excisional skin wound was created on the back of mice. Briefly, the mice were anesthetized, and betadine scrub and 70% ethanol were applied alternatively on the back three times. Full thickness skin was then excised by using a 1 cm by 1 cm template and surgical scissors. In order to apply treatments (vehicle control, empty ELP, native sRAGE, and vRAGE-ELP), fibrin gels were prepared. Briefly, 5 μM of empty ELP, native sRAGE or vRAGE-ELP were mixed in 80 μL of fibrinogen solution, which was prepared by dissolving human fibrinogen (MilliporeSigma) in deionized water at a final concentration of 6.25 mg/mL. The empty ELP and vRAGE-ELP in fibrinogen were then placed in a 37 °C water bath to initiate coacervate formation. The coacervates in fibrinogen solution were then mixed with 20 μL of thrombin at 12.5 U/mL (MilliporeSigma). The mixture was immediately applied onto the wound by pipetting and allowed to rest for 2 min to form a gel. The wound area was then covered with Tegaderm™ (3 M, USA) and photographed on days 1, 3, 7 and weekly thereafter over a period of 35 days. The percent wound closure at each time point compared to the initial wound area was analyzed using Image J software (NIH) and calculated as  $\left(1 - \frac{\text{remaining wound area}}{\text{initial wound area}}\right) \times 100$ .

**2.6.2. Wound tissue histology and epidermal thickness**—On post-wounding day 35, wounded skin samples were collected and fixed in 10% formalin for at least 24 h before processing for histology at Rutgers Research Pathology Services. Tissue samples were paraffin-embedded and thin sections (5 μm) were stained with hematoxylin and eosin (H&E) to visualize tissue morphology. Pictures of stained tissue samples on glass slides were taken using a light microscope and a microscope camera (Olympus CKX41 and Infinity 2, Lumenera). Epidermal thickness and dermal thickness were measured using ImageJ.

## 2.7. Statistical analysis

GraphPad Prism 8 software (GraphPad Software Inc., San Diego, CA, USA) was used for statistical analysis. The *p* value was calculated by using ANOVA followed by post-hoc analysis with Tukey's test to identify differences among groups at specific time points. A value of *p* < 0.05 was considered statistically significant. Results are expressed as mean ± SEM. Additionally, Kaplan Meier endpoint analysis was performed to compare the effects of empty ELP, free sRAGE and vRAGE-ELP on *in vivo* wound healing.

## 3. Results

### 3.1. vRAGE-ELP expression vector design

The design of vRAGE-ELP fusion protein is shown in Fig. 1A. The linker consisting of three repeats of four glycines and one serine, (GGGGS)<sub>3</sub> was chosen as this specific type of linker provides flexibility while allowing for mobility of the bioactive domain [29]. Genes encoding the V domain of RAGE (residues 23–123) and the linker sequence were synthesized and subcloned into ELP plasmids containing 50 pentapeptide repeats (V40C2, where V = VPGVG and C = VPGVGVPVGVPVPGCGVPGVGVPGVG) using two restriction enzyme sites, *Xba*I and *Nde*I (Fig. 1B). The predicted molecular weight of vRAGE-ELP fusion protein is 35.8



coacervate formation. In contrast, a clear signal with a single peak was shifted rightwards at 30 °C and 37 °C, thereby confirming the formation of coacervates at these temperatures. Autocorrelation analyses of the light scattering time series (Fig. 2C) show y-intercepts near one, indicating low noise from multiple scattering. Sharp transitions in the correlation coefficient track with particle size and are consistent with low polydispersity, particularly at 30 °C and 37 °C. Interestingly, the size distribution at 30 °C was broader indicating the coacervates have just begun to form. We also monitored the size of coacervates over a 7-day period and the size at 5  $\mu\text{M}$  did not significantly change (Supplementary Fig. 1).

**3.2.3. Binding of vRAGE-ELP to AGEs**—Quantification of the vRAGE-ELP binding curve showed that both vRAGE-ELP and free sRAGE bind to AGE (glycated BSA) in a similar fashion; in contrast, empty ELP did not bind AGEs. Thus, it is the vRAGE portion of vRAGE-ELP that is responsible for binding (Fig. 3A). None of vRAGE-ELP, free sRAGE or empty ELP showed noticeable binding to BSA-coated wells used as a control (Fig. 3B).

**3.2.4. Release of vRAGE-ELP monomers from coacervates**—A previous study on SDF1-ELP suggested that fusion protein-ELP coacervates co-exist with monomers at equilibrium [23,27]. Therefore, we next questioned whether the coacervate form of vRAGE-ELP releases vRAGE-ELP monomers over time, and what is the equilibrium point between monomers and coacervates. vRAGE-ELP (25  $\mu\text{M}$ ) was incubated at 37 °C and the fraction of vRAGE-ELP monomers released was measured over time. As shown in Fig. 3C, the percentage of vRAGE-ELP monomers released from the coacervates was around 17% after a 2-h incubation and this fraction for the remainder of the time course of 72 h oscillated between 18% and 21%. This suggests that, at equilibrium, 18–21% of vRAGE-ELP monomers is with coacervates.

### 3.3. In vitro bioactivity

In order to investigate the bioactivity of vRAGE-ELP in an *in vitro* simulated diabetic condition, we used cultured HUVECs, which express RAGEs [10,33,34], thus allowing the study of blockade effects of vRAGE-ELP in the presence of AGEs. In previous studies, AGE-stimulated HUVECs showed a decrease in proliferation [33], an increase in pro-inflammatory marker expression [9], and inhibition of migration [33]. Furthermore, endothelial cells are known to be involved in angiogenesis and cell proliferation during wound healing [27]. Therefore, we investigated whether vRAGE-ELP could block AGE-RAGE interaction in AGE-stimulated HUVECs.

**3.3.1. HUVEC viable number**—We stimulated HUVECs with commercially available AGEs, consisting of glycated BSA. We used 100  $\mu\text{g}/\text{mL}$  of AGEs, a concentration previously shown to decrease cell proliferation and increase pro-inflammatory marker expression [9,33]. To investigate whether vRAGE-ELP could recover the proliferation of AGE-stimulated HUVECs, we added pre-mixed AGEs with vRAGE-ELP to the cells. We also investigated dose-dependent effects of vRAGE-ELP by varying the concentration of vRAGE-ELP. Fig. 4A shows that 100  $\mu\text{g}/\text{mL}$  of AGEs alone reduced the number of HUVECs to 70% of the group treated with 100  $\mu\text{g}/\text{mL}$  non-modified BSA. When 300  $\mu\text{g}/\text{mL}$  of vRAGE-ELP were applied, cell number was slightly increased although not

statistically significant. When cells were treated with 500 µg/mL of vRAGE-ELP, cell number significantly increased compared to the AGE-stimulated group ( $p < 0.01$ ), and the effect was even more significant at 1 mg/mL of vRAGE-ELP ( $p < 0.001$ ), consistent with a dose-dependent effect of vRAGE-ELP. Therefore, we used 1 mg/mL of vRAGE-ELP in subsequent experiments. The vehicle control consisting of empty ELP did not restore cell number, which confirms that the V-domain of RAGE was responsible for the bioactivity of vRAGE-ELP. As an additional treatment control, we tested the ability of the antioxidant *N*-acetylcysteine (NAC) to knock down the AGE-mediated response [9]. Interestingly, NAC restored cell number similarly to vRAGE-ELP, suggesting that the reduced cell number in AGE-stimulated cells is a result of downstream intracellular ROS generation.

**3.3.2. ROS measurement**—As both vRAGE-ELP and NAC protected HUVECs from AGEs, we next investigated whether vRAGE-ELP reduces ROS generation in AGE-stimulated cells. There was an increase in ROS levels when HUVECs were stimulated with AGEs alone (Fig. 4B). In contrast, both vRAGE-ELP (1 mg/mL) and NAC (30 mM) decreased ROS levels in AGE-stimulated HUVECs. A vehicle control (empty ELP) did not reduce AGE-induced ROS levels, indicating that the vRAGE portion of the fusion protein is required to inhibit AGE-mediated ROS generation.

**3.3.3. Surface ICAM-1 expression**—One of the downstream cellular events resulting from AGE-RAGE binding is the upregulation of pro-inflammatory markers, including ICAM-1 [3,28]. Basal expression of ICAM-1 is low on endothelial cells, but the expression is significantly up-regulated in inflammation [35]. We investigated whether vRAGE-ELP could suppress the expression of ICAM-1. AGE-stimulated HUVECs exhibited an increased level of ICAM-1, compared to those treated with regular BSA, as seen by immunocytochemistry using anti-ICAM1 antibodies (Fig. 5A). vRAGE-ELP as well as NAC reversed the effect of AGE stimulation. As expected, vehicle control consisting of empty ELP did not have much effect on ICAM-1 levels. To quantify ICAM-1 surface expression, we also performed a cell-based ELISA (Fig. 5B). Consistent with Fig. 5A, AGEs increased ICAM-1 expression. Furthermore, when HUVECs were pre-treated with a polyclonal anti-RAGE antibody, AGEs failed to induce ICAM-1 expression, indicating that the ICAM-1 response reflects an interaction of AGEs with RAGEs on the HUVEC surface. Both the fusion protein vRAGE-ELP and NAC inhibited AGE-mediated ICAM-1 expression. There was a statistically significant difference between the AGE-stimulated and vRAGE-treated groups ( $p < 0.0001$ ), while the empty ELP, used as vehicle control, did not show much effect. Thus the inhibitory effect of vRAGE-ELP on AGE-RAGE signaling is very similar to that of the anti-RAGE blocking antibody and NAC.

**3.3.4. Stability in elastase in vitro**—While a previous study reported instability of some ELP constructs in elastase, one of the proteases found in diabetic wounds, a recent study, where the same ELP construct was used to develop SDF1-ELP, showed that SDF1-ELP remained intact up to 7 days in the presence of 1 µM elastase [23,36]. Therefore, to ensure that vRAGE-ELP would also remain intact in elastase, we conducted a stability test by incubating vRAGE-ELP or free sRAGE in elastase or in PBS without elastase at 37 °C for up to 7 days. The results shown in Fig. 6A and B indicate that vRAGE-ELP remained

intact in the presence of elastase while free sRAGE degraded after 3 days. Interestingly, free sRAGE incubated in PBS without elastase showed a weaker band on days 5 and 7 on the Western blot while vRAGE-ELP remained intact.

### 3.4. In vivo bioactivity: effects of vRAGE-ELP on wound healing in diabetic mice

To investigate the effects of vRAGE-ELP cocervates *in vivo*, we created 1 cm by 1 cm excisional wounds in diabetic mice and treated them once topically with fibrin gel, empty ELP, native sRAGE, or vRAGE-ELP. We used 5  $\mu$ M (corresponding to 20  $\mu$ g/100  $\mu$ L) of sRAGE or vRAGE-ELP, which is the dose reported in the literature where multiple doses of native sRAGE were found to improve diabetic wound healing in mice [11,12]. Fig. 7A shows images of wounded areas taken at regular time points. Wounds treated with vRAGE-ELP closed faster than any other group; this difference was especially evident starting on day 21. We quantified the percent wound closure throughout the wound healing process by taking one minus the ratio of the remaining open wound area compared to the initial wound area. As shown in Fig. 7B, mice treated with vRAGE-ELP showed significantly faster wound closure starting on day 7, with over 90% wound closure on day 28, whereas wounds in other groups were only about 60–78% closed on day 28. Although native sRAGE caused more rapid wound closure compared to the control groups, native sRAGE was generally less effective than vRAGE-ELP. Furthermore, Kaplan Meier endpoint analysis was performed to compare the effects of empty ELP, free sRAGE and vRAGE-ELP (Supplementary Fig. 2). When the time at which mice achieved 50% wound closure was set in the analysis, there was a statistically significant difference between vRAGE-ELP and empty ELP ( $p = 0.0065$ , Supplementary Fig. 2A). When the time at which mice achieved 70% wound closure was set, there was a statistically significant difference between empty ELP and free sRAGE, empty ELP and vRAGE-ELP, and free sRAGE and vRAGE-ELP ( $p = 0.01$ ,  $p = 0.001$ ,  $p = 0.018$ , respectively, Supplementary Fig. 2B). Additionally, when the time at which mice achieved 80% wound closure was set, there was a statistically significant difference between vRAGE-ELP and empty ELP, and vRAGE-ELP and free sRAGE ( $p = 0.0055$ ,  $p = 0.0136$ , respectively, Supplementary Fig. 2C).

On day 35 post-wounding, we collected skin wound tissues for histology analysis. H&E staining results show that the epidermal layer in mice treated with vRAGE-ELP was continuous throughout the section and was thicker than in the other groups (Fig. 8A). In contrast, there was no distinguishable epidermis in the middle of the wound in the fibrin-treated or vehicle control group (red arrows) confirming incomplete wound closure on day 35. Although there was visible epidermis in the native sRAGE groups, the skin layer was relatively thinner compared to the vRAGE-ELP group. We also quantified the thicknesses of epidermis and dermis in each group by randomly selecting a few spots throughout sections. Both epidermis and dermis were thicker in mice treated with vRAGE-ELP compared to the other groups (Fig. 8B–C). Mice treated with native sRAGE also showed a thicker epidermis compared to the fibrin-treated group. There was no significant difference in dermal thickness among the groups treated with fibrin, empty ELP and native sRAGE.

## 4. Discussion

The majority of therapeutic options used to improve the metabolism of chronic wounds involve enhancing the delivery of oxygen to tissue. There are no available treatments that address the impact of AGE-mediated signaling on the biological mechanisms of impaired healing in diabetes. Although sRAGE was previously reported to be effective in blocking AGE-RAGE-mediated signaling and in enhancing diabetic wound healing in experimental animals [11], potential therapeutic peptides have limited ability to survive in the presence of the high levels of proteases [11,12,22,23]. To circumvent this issue, the peptide may be administered frequently and multiple times, such as in the case of sRAGE in a mouse model, which was given daily on post-wounding days 3–10 [11]. This, however, would be costly and impractical in clinical settings. ELP-based coacervates have shown promise as delivery systems for peptide growth factors in prior studies both *in vitro* and *in vivo* [22,23,27]. Herein, we took advantage of the ELP delivery system to develop a wound protease-resistant fusion protein containing vRAGE that inhibits the binding of AGEs to RAGEs on the surface of endothelial cells, thus knocking down ROS generation and ICAM-1 expression induced by AGEs, as well as reversing the decrease in viability caused by AGEs.

The mechanism of protection from proteolysis is not well understood; our results showed that at 37 °C, which is well above the recorded transition temperature of 30–31 °C, approximately 80% of the vRAGE-ELP protein was in coacervate form and 20% was in monomeric form (or small assemblies <900 kD molecular weight cutoff of the membrane separator). It is possible that the coacervate configuration decreases the contact surface area between vRAGE and surrounding proteases; however, we cannot exclude that even monomeric vRAGE-ELP itself may be more protease-resistant. vRAGE-ELP may also be more inherently stable as it was noted that native sRAGE was lost at 37 °C even in the absence of exogenous proteases *in vitro* (Fig. 6). We chose a 7-day incubation period to evaluate stability in elastases as wound dressings are often replaced on a weekly basis; thus, vRAGE-ELP would not be expected to lose activity in-between dressing changes. Although the diabetic wound fluid generally exhibits significant levels of MMP-2, MMP-9 and elastase, the levels of proteases may vary depending on wound etiology, healing stage and bacterial colonization. A wider range of wound fluid samples would be necessary to fully assess the stability of vRAGE-ELP in the wound environment.

vRAGE-ELP reversed the effect of AGEs on three different responses in HUVECs: (1) increased ROS levels, (2) increased ICAM-1 expression, and (3) decreased viability. The vehicle control consisting of empty ELPs showed no effect confirming it is vRAGE that retains the biological effect of the molecule. A dose-dependent effect of vRAGE-ELP was observed, with a return to baseline level using 1 mg/mL vRAGE-ELP (~28 µM) in the viability/proliferation assay in presence of 100 µg/mL AGEs (~1.4 µM) while 300 µg/mL vRAGE-ELP (~8.4 µM) did not show a significant difference, suggesting there may be a minimal amount of vRAGE-ELP required to be effective as a competitive inhibitor. This finding is also consistent with previous findings where 30 times molar excess of sRAGE were used to study the blockade effects of sRAGE when AGEs were present [9]. Furthermore, the antioxidant NAC mimicked the effect of vRAGE-ELP based on these three metrics. Previous studies have shown that NAC can inhibit inflammation *in vitro* and

improve wound healing in diabetic mice [37,38]; while NAC is widely available, it is not used in clinical settings for treating wounds. NAC is not a specific antioxidant, and it is unclear whether it would still be beneficial in a typical wound environment where ROS are potentially important for signaling immune cell recruitment and in mechanisms to kill pathogens [39]. The use of anti-RAGE antibodies in the ICAM-1 expression studies also suggests that blocking RAGEs is a potential alternative to prevent binding AGEs (Fig. 5B). A prior study showed that anti-RAGE antibody-applied wounds in diabetic mice healed faster compared with a control group [40]. However, in that study, anti-RAGE antibodies were applied every two days until post-wounding day 10 implying the *in vivo* use of antibodies may be costly, and their effectiveness may be compromised by wound proteases.

We used a genetically induced diabetic mouse model to investigate the bioactivity of vRAGE-ELP *in vivo*. Although the time scale of onset of diabetes in these animals is on the order of weeks as compared to years and decades in humans, wounds in diabetic mice are widely used to study diabetic impaired wound healing [41,42], as well as to carry out initial evaluations of potential therapeutics such as sRAGE and other ELP fusion proteins [11,21–23,27]. Furthermore, high levels of AGEs are found in diabetic mice [41], and RAGE expression is down-regulated in wounds of diabetic mice treated by sRAGE [11], thus making it an ideal system to study the impact of AGE-mediated signaling, and its inhibition thereof, on wound healing. Mice treated with a single dose of vRAGE-ELP closed excisional skin wounds faster than any other group, including those treated with native sRAGE, as well as the control groups treated with fibrin or vehicle (empty ELP) (Fig. 7). Wound closure in the vRAGE-ELP-treated group appeared to be one week ahead compared to the sRAGE-treated group, and two weeks ahead compared to the vehicle control. Consistent with this observation, vRAGE-ELP treatment also resulted in thicker epidermis and dermis, suggesting a more mature scar (Fig. 8). Prior studies with sRAGE have suggested that inhibiting AGE-mediated signaling decreases the levels of inflammatory markers in mouse diabetic wounds [9,11]. Based on the *in vitro* data included herein, a similar mechanism is potentially involved with vRAGE-ELP but it would have to be explored *in vivo* in the future.

## 5. Conclusions

In conclusion, we report that a novel vRAGE-ELP fusion protein inhibits AGE-RAGE mediated signaling and enhances wound healing in diabetic mice. vRAGE-ELP reversibly form coacervates ranging in size from 500 to 1600 nm. To our knowledge, this is the first study where a competitive inhibitor of AGE, namely vRAGE, was engineered in the form of fusion proteins, which provide a stable form of delivery method for vRAGE in the highly proteolytic wound environment. Our results suggest that vRAGE-ELP reversed the effects of AGE-RAGE-mediated signaling *in vitro* and that one dose of vRAGE-ELP treatment was effective to accelerate wound healing in diabetic mice, compared to control vehicle groups. Furthermore, the small size of vRAGE-ELP coacervates would make it possible to incorporate them into already existing microporous skin substitutes and hydrogels currently used clinically.

## Supplementary Material

Refer to Web version on PubMed Central for supplementary material.

## Acknowledgements

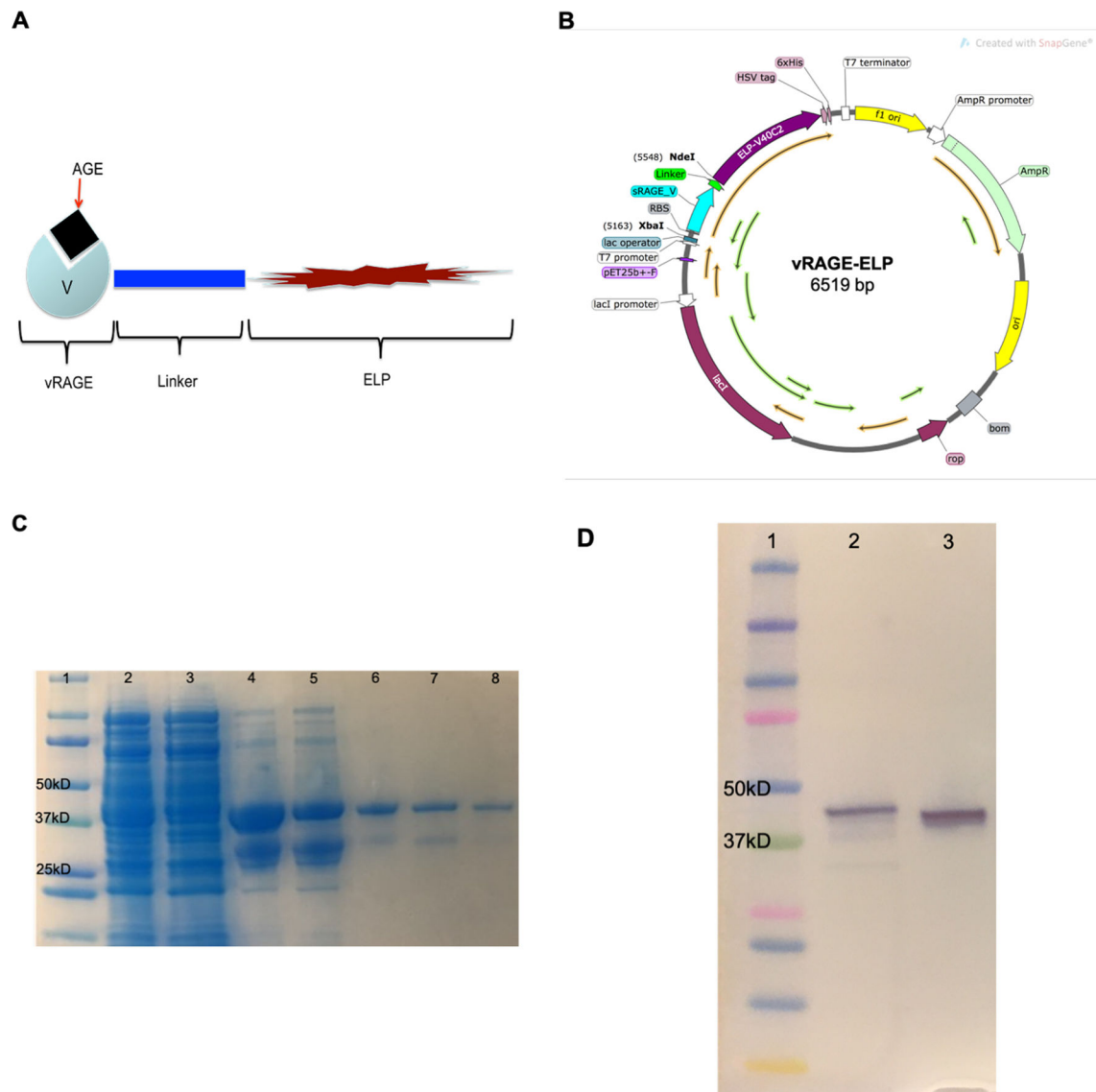
This work was supported by a National Institutes of Health Grant (R21EB021570).

## References

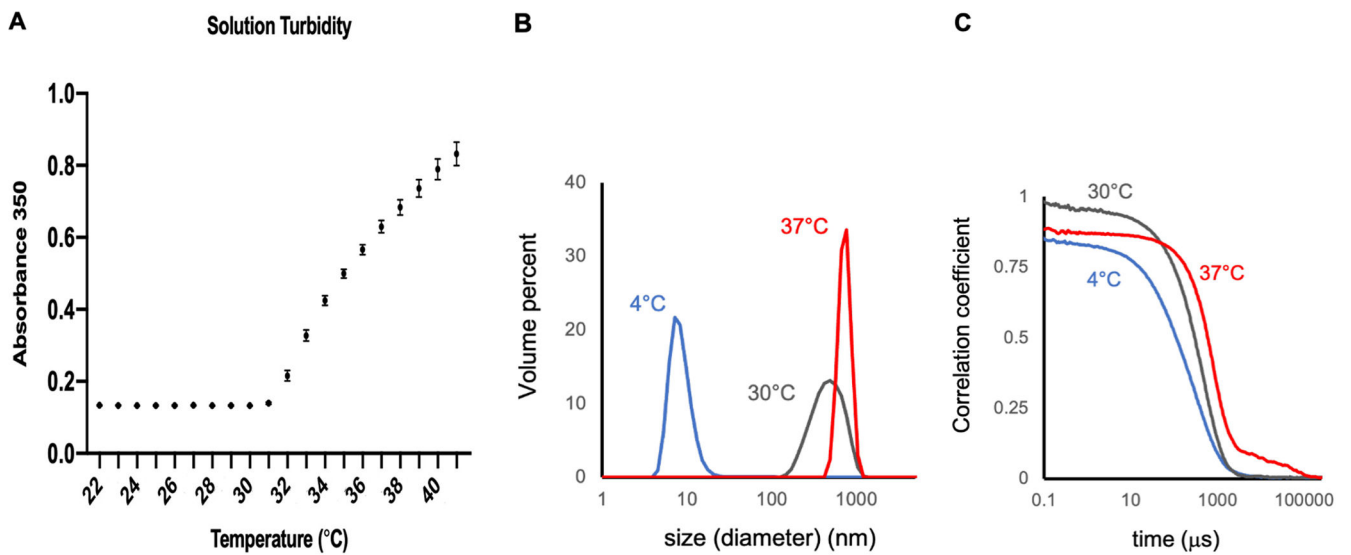
- [1]. Sen CK, Human wounds and its burden: an updated compendium of estimates, *Adv. Wound Care (New Rochelle)* 8 (2) (2019) 39–48. [PubMed: 30809421]
- [2]. Nussbaum SR, Carter MJ, Fife CE, DaVanzo J, Haught R, Nusgart M, et al. , An economic evaluation of the impact, cost, and Medicare policy implications of chronic nonhealing wounds, *Value Health* 21 (1) (2018) 27–32. [PubMed: 29304937]
- [3]. Ahmed N, Advanced glycation endproducts–role in pathology of diabetic complications, *Diabetes Res. Clin. Pract* 67 (1) (2005) 3–21. [PubMed: 15620429]
- [4]. Goldin A, Beckman JA, Schmidt AM, Creager MA, Advanced glycation end products: sparking the development of diabetic vascular injury, *Circulation*. 114 (6) (2006) 597–605. [PubMed: 16894049]
- [5]. Hu SC, Lan CE, High-glucose environment disturbs the physiologic functions of keratinocytes: focusing on diabetic wound healing, *J. Dermatol. Sci* 84 (2) (2016) 121–127. [PubMed: 27461757]
- [6]. Brownlee M, Biochemistry and molecular cell biology of diabetic complications, *Nature*. 414 (2001) 813–820. [PubMed: 11742414]
- [7]. Barnes P, Karin M, Nuclear factor- $\kappa$ B - a pivotal transcription factor in chronic inflammatory disease, *N. Engl. J. Med* 336 (15) (1997) 1066–1071. [PubMed: 9091804]
- [8]. Liu T, Zhang L, Joo D, et al. , NF- $\kappa$ B signaling in inflammation, *Sig. Transduct. Target Ther* 2 (2017) 17023.
- [9]. Schmidt AMHO, Chen JX, Li JF, Crandall J, Zhang J, Cao R, Yan SD, Brett J, Stern D, Advanced glycation endproducts interacting with their endothelial receptor induce expression of vascular cell adhesion molecule-1 (VCAM-1) in cultured human endothelial cells and in mice, *J. Clin. Invest* 96 (1995) 1395–1403. [PubMed: 7544803]
- [10]. Kislinger TFC, Huber B, Qu W, Taguchi A, Yan S, Hofmann M, Yan S, Pischetsrieder M, Stern D, Schmidt A, Ne-(Carboxymethyl)lysine adducts of proteins are ligands for receptor for advanced glycation end products that activate cell signaling pathways and modulate gene expression, *J. Biol. Chem* 274 (44) (1999) 31740–31749. [PubMed: 10531386]
- [11]. Goova MT, Li J, Kislinger T, Qu W, Lu Y, Bucciarelli LG, et al. , Blockade of receptor for advanced glycation end-products restores effective wound healing in diabetic mice, *Am. J. Pathol* 159 (2) (2001) 513–525. [PubMed: 11485910]
- [12]. Olekson MP, Faulknor RA, Hsia HC, Schmidt AM, Berthiaume F, Soluble receptor for advanced glycation end products improves stromal cell-derived Factor-1 activity in model diabetic environments, *Adv. Wound Care (New Rochelle)* 5 (12) (2016) 527–538. [PubMed: 28078186]
- [13]. Schmidt AMSDM, RAGE: A new target for the prevention and treatment of the vascular and inflammatory complications of diabetes, *TEM*. 11 (9) (2000) 368–375. [PubMed: 11042467]
- [14]. Bongarzone S, Savickas V, Luzi F, Gee AD, Targeting the receptor for advanced glycation Endproducts (RAGE): A medicinal chemistry perspective, *J. Med. Chem* 60 (17) (2017) 7213–7232. [PubMed: 28482155]
- [15]. Xue J, Rai V, Singer D, Chabierski S, Xie J, Reverdatto S, et al. , Advanced glycation end product recognition by the receptor for AGEs, *Structure*. 19 (5) (2011) 722–732. [PubMed: 21565706]
- [16]. Matsumoto SYT, Murata H, Harada S, Fujita N, Nakamura S, Yamamoto Y, Watanabe T, Yonekura H, Yamamoto H, Ohkubo T, Kobayashi Y, Solution structure of the variable-type

- domain of the receptor for advanced glycation end products: new insight into AGE-RAGE interaction, *Biochemistry*. 47 (2008) 12299–12311. [PubMed: 19032093]
- [17]. Tardaguila-Garcia A, Garcia-Morales E, Garcia-Alamino JM, Alvaro-Afonso FJ, Molines-Barroso RJ, Lazaro-Martinez JL, Metalloproteinases in chronic and acute wounds: A systematic review and meta-analysis, *Wound Repair Regen*. 27 (4) (2019) 415–420. [PubMed: 30873727]
- [18]. Guo S, Dipietro LA, Factors affecting wound healing, *J. Dent. Res* 89 (3) (2010) 219–229. [PubMed: 20139336]
- [19]. Chilkoti A, Dreher MR, Meyer DE, Design of thermally responsive, recombinant polypeptide carriers for targeted drug delivery, *Adv. Drug Deliv. Rev* 54 (2002) 1093–1111. [PubMed: 12384309]
- [20]. Despanie J, Dhandhukia JP, Hamm-Alvarez SF, MacKay JA, Elastin-like polypeptides: therapeutic applications for an emerging class of nanomedicines, *J. Control. Release* 240 (2016) 93–108. [PubMed: 26578439]
- [21]. Devalliere J, Dooley K, Hu Y, Kelangi SS, Uygun BE, Yarmush ML, Co-delivery of a growth factor and a tissue-protective molecule using elastin biopolymers accelerates wound healing in diabetic mice, *Biomaterials*. 141 (2017) 149–160. [PubMed: 28688286]
- [22]. Koria P, Yagi H, Kitagawa Y, Megeed Z, Nahmias Y, Sheridan R, et al. , Self-assembling elastin-like peptides growth factor chimeric nanoparticles for the treatment of chronic wounds, *Proc. Natl. Acad. Sci. U. S. A* 108 (3) (2011) 1034–1039. [PubMed: 21193639]
- [23]. Yeboah A, Cohen RI, Faulknor R, Schloss R, Yarmush ML, Berthiaume F, The development and characterization of SDF1 $\alpha$ -elastin-like-peptide nanoparticles for wound healing, *J. Control. Release* 232 (2016) 238–247. [PubMed: 27094603]
- [24]. McDaniel JR, Callahan DJ, Chilkoti A, Drug delivery to solid tumors by elastin-like polypeptides, *Adv. Drug Deliv. Rev* 62 (15) (2010) 1456–1467. [PubMed: 20546809]
- [25]. Meyer DECA, Purification of recombinant proteins by fusion with thermally-responsive polypeptides, *Nat. Biotechnol* 17 (1999) 1112–1115. [PubMed: 10545920]
- [26]. Hassouneh W, MacEwan SR, Chilkoti A, Fusions of elastin-like polypeptides to pharmaceutical proteins, *Methods Enzymol*. 502 (2012) 215–237. [PubMed: 22208987]
- [27]. Yeboah A, Maguire T, Schloss R, Berthiaume F, Yarmush ML, Stromal cell-derived growth Factor-1  $\alpha$ -elastin like peptide fusion protein promotes cell migration and revascularization of experimental wounds in diabetic mice, *Adv. Wound Care (New Rochelle)* 6 (1) (2017) 10–22. [PubMed: 28116224]
- [28]. Guo ZJ, Niu HX, Hou FF, Zhang L, Fu N, Nagai R, et al. , Advanced oxidation protein products activate vascular endothelial cells via a RAGE-mediated signaling pathway, *Antioxid. Redox Signal* 10 (10) (2008) 1699–1712. [PubMed: 18576917]
- [29]. Chen X, Zaro JL, Shen WC, Fusion protein linkers: property, design and functionality, *Adv. Drug Deliv. Rev* 65 (10) (2013) 1357–1369. [PubMed: 23026637]
- [30]. Brito LA, Singh M, Acceptable levels of endotoxin in vaccine formulations during preclinical research, *J. Pharm. Sci* 100 (1) (2011) 34–37. [PubMed: 20575063]
- [31]. Schwarz H, Schmittner M, Duschl A, Horejs-Hoek J, Residual endotoxin contaminations in recombinant proteins are sufficient to activate human CD1c<sup>+</sup> dendritic cells, *PLoS One* 9 (12) (2014), e113840. [PubMed: 25478795]
- [32]. Christensen T, Hassouneh W, Trabbic-Carlson K, Chilkoti A, Predicting transition temperatures of elastin-like polypeptide fusion proteins, *Biomacromolecules*. 14 (5) (2013) 1514–1519. [PubMed: 23565607]
- [33]. Li Y, Chang Y, Ye N, Dai D, Chen Y, Zhang N, et al. , Advanced glycation end products inhibit the proliferation of human umbilical vein endothelial cells by inhibiting Cathepsin D, *Int. J. Mol. Sci* 18 (2) (2017).
- [34]. Xiong F, Leonov S, Howard AC, Xiong S, Zhang B, Mei L, et al. , Receptor for advanced glycation end products (RAGE) prevents endothelial cell membrane resealing and regulates F-actin remodeling in a beta-catenin-dependent manner, *J. Biol. Chem* 286 (40) (2011) 35061–35070. [PubMed: 21844192]

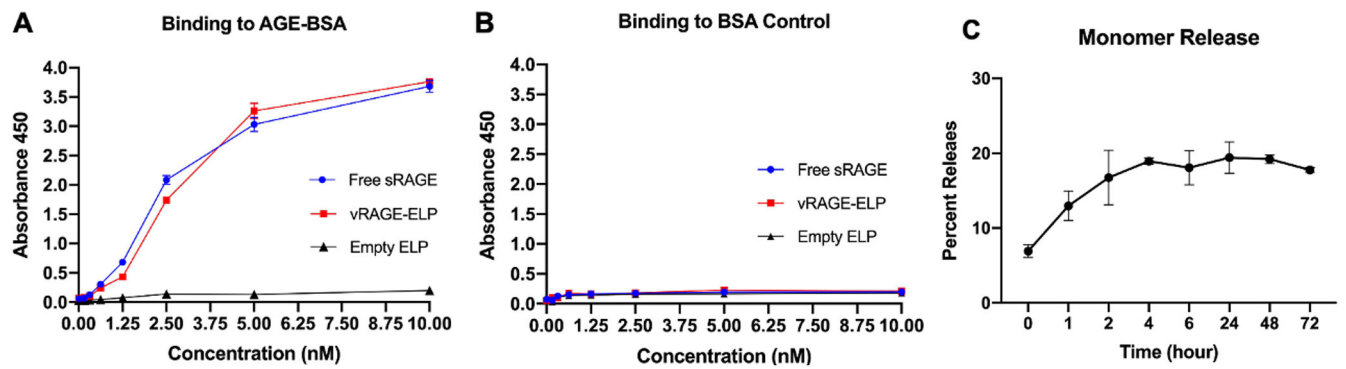
- [35]. Wiesolek HL, Bui TM, Lee JJ, Dalal P, Finkielstein A, Batra A, et al. , Intercellular adhesion molecule 1 functions as an Efferocytosis receptor in inflammatory macrophages, *Am. J. Pathol* 190 (4) (2020) 874–885. [PubMed: 32035057]
- [36]. Shah M, Hsueh PY, Sun G, Chang HY, Janib SM, MacKay JA, Biodegradation of elastin-like polypeptide nanoparticles, *Protein Sci.* 21 (6) (2012) 743–750. [PubMed: 22434766]
- [37]. Ayuk SM, Abrahamse H, Houreld NN, The role of matrix metalloproteinases in diabetic wound healing in relation to Photobiomodulation, *J. Diabetes Res* 2016 (2016) 2897656. [PubMed: 27314046]
- [38]. Park JH, Kang SS, Kim JY, Tchah H, The antioxidant N-acetylcysteine inhibits inflammatory and apoptotic processes in human conjunctival epithelial cells in a high-glucose environment, *Invest. Ophthalmol. Vis. Sci* 56 (9) (2015) 5614–5621. [PubMed: 26305534]
- [39]. Dunnill C, Patton T, Brennan J, Barrett J, Dryden M, Cooke J, et al. , Reactive oxygen species (ROS) and wound healing: the functional role of ROS and emerging ROS-modulating technologies for augmentation of the healing process, *Int. Wound J* 14 (1) (2017) 89–96. [PubMed: 26688157]
- [40]. Wang Q, Zhu G, Cao X, Dong J, Song F, Niu Y, Blocking AGE-RAGE signaling improved functional disorders of macrophages in diabetic wound, *J. Diabetes Res* 2017 (2017) 1428537. [PubMed: 29119117]
- [41]. Hansen LM, Gupta D, Joseph G, Weiss D, Taylor WR, The receptor for advanced glycation end products impairs collateral formation in both diabetic and non-diabetic mice, *Lab. Investig* 97 (1) (2017) 34–42. [PubMed: 27869797]
- [42]. Parnell LKS, Volk SW, The evolution of animal models in wound healing research: 1993–2017, *Adv. Wound Care (New Rochelle)* 8 (12) (2019) 692–702. [PubMed: 31827981]

**Fig. 1.**

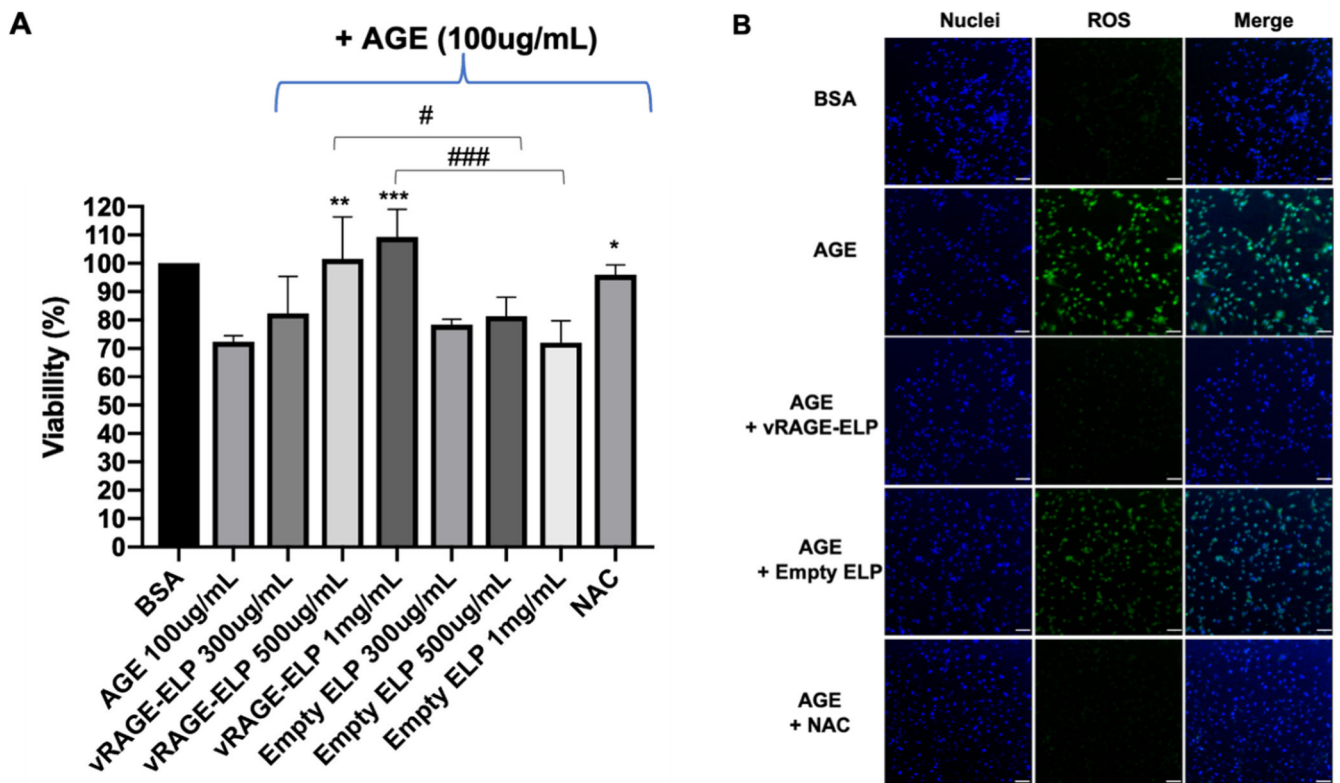
Expression and Purification of vRAGE-ELP. (A) Design of vRAGE-ELP fusion protein. The V domain of RAGE was fused to 50 repeats of ELP *via* a 15-amino acid linker. (B) Plasmid map of vRAGE-ELP expression vector. Genes encoding the V domain of RAGE and the linker were subcloned into the ELP plasmid using *XbaI* and *NdeI* restriction enzymes. The plasmid map was created using SnapGene software (from Insightful Science; available at [snapgene.com](http://snapgene.com)). (C) SDS-PAGE of product after each purification step. A clear band in the final product was observed (lane 8). Lane 1: Protein standard, Lane 2: Total lysate, Lane 3: Supernatant collected after the 1st hot spin, Lane 4: Supernatant collected after the 1st cold spin, Lane 5: Supernatant collected after the 2nd hot spin, Lane 6: Supernatant collected after the 2nd cold spin, Lane 7: Supernatant collected after the 3rd hot spin, Lane 8: Supernatant collected after the 3rd cold spin, which is the final product. (D) Western blot analysis of final product. Lane 1: Protein standard ladder, Lane 2: Native sRAGE as a control, Lane 3: vRAGE-ELP final product.



**Fig. 2.** Transition temperature and size of coacervates. (A) Solution turbidity of vRAGE-ELP fusion proteins. The solution turbidity increases after around 30 °C indicating the formation of coacervates.  $N = 5$ . (B) Size of vRAGE-ELP coacervates at 5  $\mu\text{M}$ . The size of coacervates significantly increased as temperature increased from 4 °C to 30 °C and 37 °C. (C) Correlogram. Autocorrelation analyses of the light scattering time series show y-intercepts near one, indicating low noise from multiple scattering. Sharp transitions in the correlation coefficient track with particle size and are consistent with low polydispersity, particularly at 30 °C and 37 °C.



**Fig. 3.** Binding activity of vRAGE-ELP to AGE (A, B) and release of vRAGE-ELP monomers from vRAGE-ELP coacervates (C). (A) Binding to AGE. vRAGE-ELP and sRAGE showed similar binding activities to AGE while empty ELP did not bind to AGE. (B) Binding to BSA as a control. None of vRAGE-ELP, free sRAGE or empty ELP showed noticeable binding to BSA control. (C) Release of vRAGE-ELP monomers from coacervates over time. Monomers were separated from coacervates using a 300–900 kD ultrafiltration membrane after incubation up to 72 h. The concentration in filtrate (monomers) was quantified using a BCA assay. Beyond 2 h of incubation, the percentage of vRAGE-ELP monomers released from the coacervates remained between 18% and 21%.  $N = 4$ .

**Fig. 4.**

Effect of AGEs and RAGEs inhibitors on HUVEC number and ROS generation. (A) Viable cell number. Viable cell number was measured after 24 h of incubation in each condition and normalized to the BSA control = 100%. AGEs alone significantly decreased cell number ( $p = 0.0147$ ). vRAGE-ELP, but not empty ELP, restored cell viability in a dose-dependent manner. NAC, an antioxidant, also recovered cell viability.  $N = 6$ . Statistics: One-way ANOVA followed by Tukey's test: # $p < 0.05$ , ### $p < 0.001$ , \* $p < 0.05$ , \*\* $p < 0.01$ , \*\*\* $p < 0.001$ . Asterisks indicate comparisons with AGE group. (B) ROS levels. AGE stimulation increased ROS generation in HUVECs. The ROS level significantly decreased when cells were treated vRAGE-ELP or NAC, while empty ELPs had no effect. AGE = 100  $\mu\text{g/mL}$ , vRAGE-ELP = 1 mg/mL, ELP = 1 mg/mL, NAC = 30 mM. Blue: Nuclei, Green: ROS. Scale bar = 200  $\mu\text{m}$ .

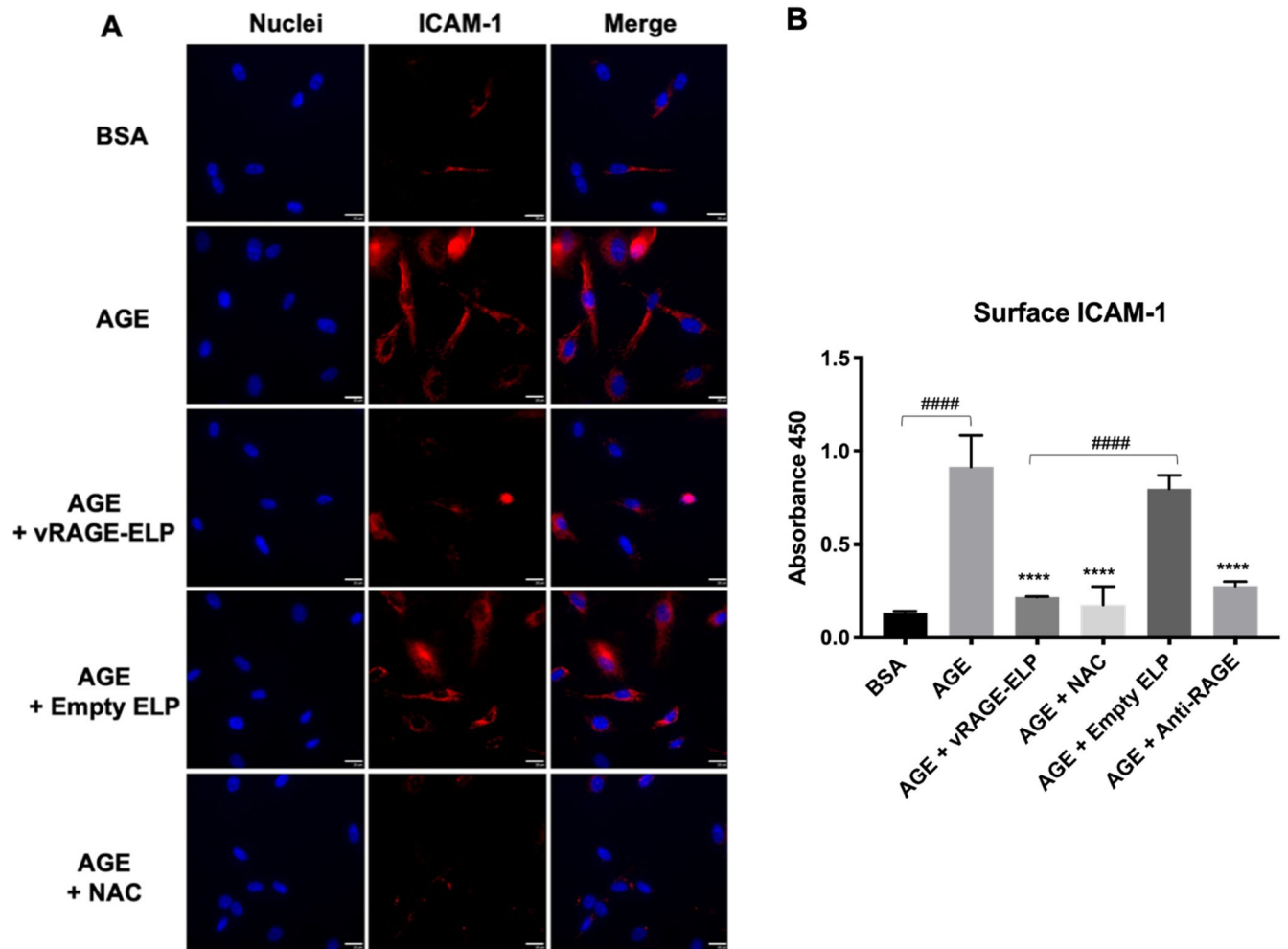


**Fig. 5.** Effect of AGEs and RAGEs inhibitors on surface ICAM-1 expression. (A) Images of immunostaining. vRAGE-ELP coacervates suppressed ICAM-1 expression in AGE-stimulated cells. Blue: DAPI-stained nuclei. Red: antibody-stained ICAM-1. Scale bar = 20  $\mu\text{m}$ . (B) Cell-based ELISA. vRAGE-ELP significantly reduced the expression of ICAM-1 ( $p < 0.0001$ ).  $N = 6$ . Statistics: One-way ANOVA, Tukey's test. ####  $p < 0.0001$ , \*\*\*\*  $p < 0.0001$ . Asterisks indicate comparisons with AGE group. BSA = 100  $\mu\text{g/mL}$ . AGE = 100  $\mu\text{g/mL}$ . vRAGE-ELP = 1  $\text{mg/mL}$ . Empty ELP = 1  $\text{mg/mL}$ . NAC = 30  $\text{mM}$ . Anti-RAGE antibody = 10  $\mu\text{g/mL}$ .

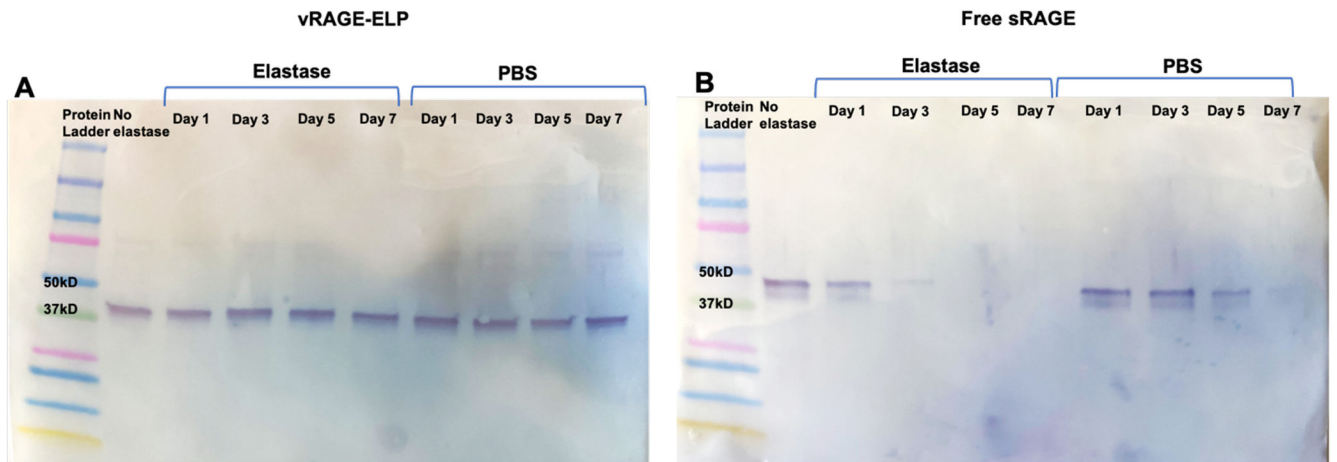


**Fig. 6.** Stability of vRAGE-ELP in elastase. (A) Western blot image of vRAGE-ELP incubated in PBS with or without elastase. vRAGE-ELP remained intact in elastase or in PBS without elastase for 7 days. (B) Western blot image of free sRAGE incubated in PBS with or without elastase. Free sRAGE showed a faint band on day 3 and no visible band on day 7 in elastase. Free sRAGE incubated in PBS also showed weaker bands after day 5.

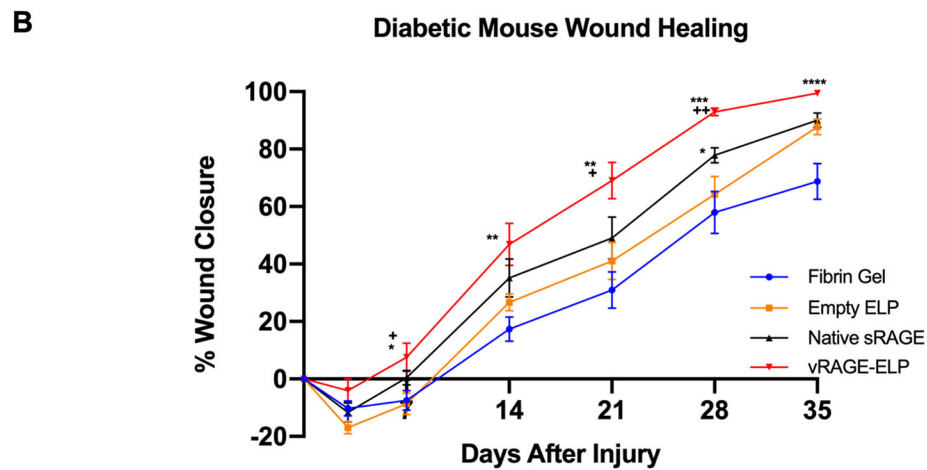


**Fig. 7.** Effect of vRAGE-ELP on skin wound closure in diabetic mice. (A) Photos of wounded areas over time. (B) Percent wound closure analyzed by comparing remaining wound areas with initial wound areas. Diabetic mice treated with vRAGE-ELP showed significantly faster wound closure compared to other groups.  $N = 8$ . Statistics: One-way ANOVA followed by Tukey's test. Asterisks (\*) indicate comparisons with fibrin gel control. Plus (+) marks indicate comparisons with vehicle (empty ELP) control. Day 7, \*  $p < 0.05$ , +  $p < 0.05$ . Day 14, \*\*  $p < 0.01$ . Day 21, \*\*  $p < 0.01$ , +  $p < 0.05$ . Day 28, \*  $p < 0.05$ , \*\*\*  $p < 0.001$ , ++  $p < 0.01$ . Day 35, \*\*\*\*  $p < 0.0001$ .

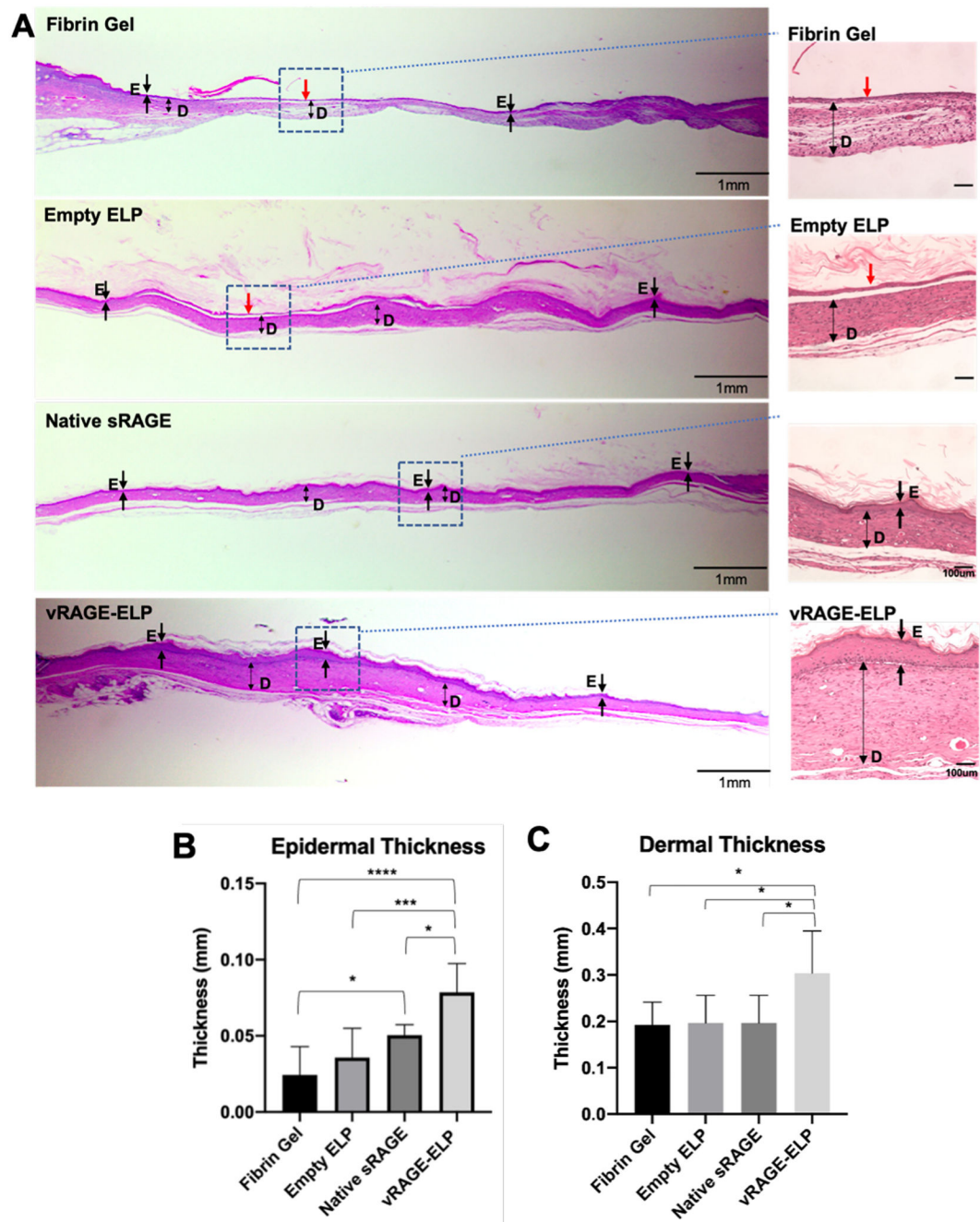


**Fig. 8.** Histology of wounded areas collected on post-wounding day 35. (A) Images from H&E staining. Single-headed arrows indicate epidermis. Double-headed arrows represent dermis. A red arrow indicates an area where no visible epidermis is observed. D: Dermis. E: Epidermis. (B) Thickness of epidermis. Values are averages of 6 randomly selected areas from two different sections per group. (C) Thickness of dermis. Values are averages of 6 randomly selected areas from two different sections per group. Statistics: One-way ANOVA followed by Tukey's test. \* $p < 0.05$ , \*\*\* $p < 0.001$ , \*\*\*\* $p < 0.0001$ .